**Liquid Crystals**
Publication details, including instructions for authors and subscription information:
http://www.informaworld.com/smpp/title~content=t713926090

# Density studies on various smectic liquid crystals

R. Kiefer[a]; G. Baur[a]
[a] Fraunhofer-Institut für Angewandte Festkörperphysik, Freiberg, F. R. Germany

**To cite this Article** Kiefer, R. and Baur, G.(1990) 'Density studies on various smectic liquid crystals', Liquid Crystals, 7: 6, 815 — 837
**To link to this Article: DOI:** 10.1080/02678299008033842
**URL:** http://dx.doi.org/10.1080/02678299008033842

LIQUID CRYSTALS, 1990, VOL. 7, NO. 6, 815–837

# Density studies on various smectic liquid crystals

by R. KIEFER and G. BAUR
Fraunhofer-Institut für Angewandte Festkörperphysik, Eckerstrasse 4,
D-7800 Freiberg, F.R. Germany

(*Received 11 July 1989; accepted 5 January 1990*)

Density measurements as a function of temperature for four homologues of the 5-*n*-alkyl-2-(4-*n*-alkyloxy-phenyl)-pyrimidines (PYP *n*O*m*) which exhibit nematic, smectic A and smectic C phases are reported. Furthermore 1-butyl-*c*-4-(4′-octylbiphenyl-4-yl)-*r*-1-cyclo-hexan-carbonitrile (NCB84) is studied; this has additionally a smectic G phase. From these data the thermal expansion coefficients are calculated. Comparing PYP 907 and PYP 709, differing in their exchanged alkyl chains, we observe in the smectic A and the smectic C phase a distinctly lower density for PYP 709 whereas their densities nearly agree in the isotropic phase. The pyrimidines PYP 709 and PYP 808 exhibit a continuous volume change on crossing the smectic A–smectic C transition which differs dramatically from PYP 909 which shows a small volume jump. Furthermore a binary mixture of PYP 708 and PYP 706 is analysed which shows only a nematic and a smectic C phase. The associated phase transition is probably first order revealing nearly no pretransitional behaviour. The smectic A–smectic C transition of NCB84 seems to be second order exhibiting a continuous change of volume across the transition whereas the smectic C–smectic G transition shows a volume discontinuity and is first order. In order to induce ferroelectric smectic C* phases all smectic C materials were doped with a chiral pyrimidine dopant. Astonishingly the thermal expansion coefficient across the smectic A–smectic C* transition is influenced by the dopant in a very different way.

## 1. Introduction

From a fundamental point of view the interest concerning the nature of the smectic C–smectic A ($S_C$–$S_A$) phase transition has grown steadily since de Gennes suggested that this transition may be continuous by symmetry reasons and proposed an analogy with superfluid helium [1]. The development of displays containing chiral smectic C ($S_C^*$) materials has further reinforced and stimulated research efforts on the $S_A$–$S_C^*$ as well as $S_C^*$-cholesteric ($S_C^*$–Ch) [2]. Up to now all of these phase transitions have been analysed mainly by calorimetric studies [3–10]. Investigations of the associated density changes, however, are very scarce [11–18]. Very useful complementary information can be obtained if the density measurements are carried out with high precision [19]. In this paper we report density studies of various homologues of the 5-*n*-alkyl-2-(4-*n*-alkyloxy-phenyl)-pyrimidines (PYP *n*O*m*) possessing nematic, $S_A$ and $S_C$ phases [20]. Furthermore 1-butyl-*c*-4-(4′-octylbiphenyl-4-yl)-*r*-1-cyclo-hexan-carbonitrile (NCB84) was studied and this shows additionally a $S_G$ phase [21]. There exists experimental evidence that the $S_C^*$–$S_A$ transition is mainly driven by intermolecular forces producing the $S_C$ phase and not by the ferroelectric coupling between the permanent dipoles. The spontaneous polarization is thus rather a secondary than a primary order parameter and the energy associated with the interaction between permanent dipoles represents only a small perturbation of the system [22, 23]. Thus a strong similarity between the $S_C$–$S_A$ and the $S_C^*$–$S_A$ phase transition would be expected at least if materials are used which possess small spontaneous polarizations as in the case of our compounds. In order to induce ferroelectric phases and to look for its volumetric properties all $S_C$ materials were doped with a chiral pyrimidine guest dopant. The associated density changes were measured and the results are discussed.

## 2. Experimental

Measurements were made with the familiar PARR digital precision density meter system (DMA 60 + 2 × DMA 602 HT) which counts the resonance frequency of a hollow glass tube filled with the liquid-crystalline material to be studied. A second measuring cell filled with *n*-nonane is used, working as a reference cell. The temperature in the cell was measured by a platinum resistance (Pt 100) placed as near as possible to the measuring cell and a Fluke 2180A RTD digital thermometer. The measured average temperature fluctuation in the temperature range of 10°C–80°C was typically smaller than 5 mK by averaging over 10 single values. The measuring signal from the *n*-nonane filled cell was taken as the reference signal for the measurement of liquid crystals. The temperatures of both measuring cells were regulated parallelly by a water filled circulation thermostat (Hake F3). Correlated temperature fluctuations occurring in both cells due to the temperature regulation procedure have a considerably reduced influence on the density values because *n*-nonane and the liquid-crystalline materials have very similar thermal expansion coefficients (except at phase transitions where a strong change of the expansion coefficient occurs). The relative precision of the evaluated density data is increased considerably by this method and should be better than $5 \times 10^{-6}$. The high sensitivity can be fully exploited by probing phase transitions with small volume changes such as $S_C$–$S_A$ transitions. The whole measuring system is fully computer controlled enabling us to evaluate automatically the density (or molar volume $V$) as a function of temperature. From these data the thermal isobaric expansion coefficient

$$\alpha = (1/V)dV/dT$$

has been calculated by numerical differentiation.

The measuring procedure is as follows. Starting generally a great distance away from the nematic–isotropic phase transition $T_{NI}$ in the isotropic region the temperature interval between successive data points amounts to a maximum value of 2°C. On approaching $T_{NI}$ this difference is diminished discontinuously until a minimum value of 0·08°C is reached at $T_{NI}$. After passing $T_{NI}$ the temperature interval is increased again in the nematic phase until it saturates at a maximum value of 2°C. If further phase transitions exist the procedure is repeated again for each transition.

Figure 1 shows the schematic structures and phase transitions of the investigated pyrimidine homologues, the binary mixture PYP 708/706, the three core compound NCB 84 as well as the chiral pyrimidine dopant PYP A62Cl. To our knowledge precise transition data of homologues of the pyrimidines, which were first synthesized by Zaschke [20], are not available in the literature. All of the compounds were supplied as a gift by the E. Merck company. The purity of the different components as determined by gas chromatography are given in brackets: PYP 706, PYP 708, PYP 808, PYP 907 and PYP A62Cl (99·9 per cent), PYP 909 (99·8 per cent), PYP 709 (99·6 per cent) and NCB 84 (99·5 per cent). The melting points were determined with a Perkin–Elmer DSC 2 calorimetric system [24]. All of the other transitions were obtained with a Leitz polarizing microscope and a Mettler hot stage.

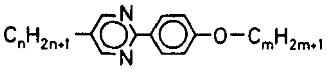

PYP-*n*O*m*

| | |
|---|---|
| PYP 909 | K 34 $S_C$ 61·0 $S_A$ 74·0 I |
| PYP 808 | K 35 $S_C$ 56·2 $S_A$ 62·8 N 68·9 I |
| PYP 907 | K 35 $S_C$ 50·5 $S_A$ 70·6 I |
| PYP 709 | K 47·5 $S_C$ 50·2 $S_A$ 56·2 N 69·2 I |
| 48% PYP 708<br>+52% PYP 706 | K 26 $S_C$ 36·0 N 69·3 I |

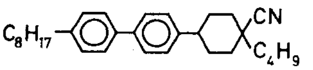

| | |
|---|---|
| NCB 84 | K 42 $S_G$ 47·9 $S_C$ 70·4 $S_A$ 87·1 N 117·2 I |

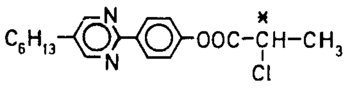

| | |
|---|---|
| PYP A62Cl | K 84 I |

Figure 1. Schematic chemical structure and transition temperatures of the liquid-crystalline compounds PYP 909, PYP 808, PYP 907, PYP 709, 48% PYP 708 + 52% PYP 706 (by weight %), and NCB84. In addition the structure of the chiral dopant PYP A62Cl is included.

## 3. Results and discussion

### 3.1. *Comparison of the pyrimidine homologues PYP 909 and PYP 907*

The molar volume of PYP 907 as well as those from PYP 709, PYP 808 and PYP 907 are given in figures 2 and 3, respectively. Evidently the molar volume of PYP 909 is distinctly larger than that of PYP 907. Yet the relative volume jumps $\Delta V/V_{S_A I}$ of the $S_A$–isotropic phase transition are comparable and amount to 1·37 per cent for PYP 909 and 1·35 per cent for PYP 907. The corresponding thermal expansion coefficients of these pyrimidine homologues are depicted in figures 4 (*a*) and (*b*). In both figures we see the narrow, large peak of the $S_A$–isotropic transition accompanied by strong pretransitional behaviour in the $S_A$ as well as in the isotropic phase. An additional small peak is observed in figure 4 (*a*) indicating the $S_C$–$S_A$ transition of PYP 909. Figure 6 (*a*) shows once more this volume change across the $S_C$–$S_A$ transition on a larger scale. The broken straight lines in the figure indicate that the volume changes per unit temperature in the $S_C$ and the $S_A$ phase nearly agree in the neighbourhood of the phase transition and we can associate to this transition a small relative volume jump $\Delta V/V_{S_C S_A}$ of about $2 \times 10^{-3}$ per cent. The transition does not appear sharply which may be caused by our low temperature resolution; but a coexistence region of $S_C$ and $S_A$ phases could not be found by microscopic observation. So we have to assume that the transition is second order. In comparison to PYP 909 the analogous $S_C$–$S_A$ transition of PYP 907 is hardly detectable in figure 4 (*b*) and the

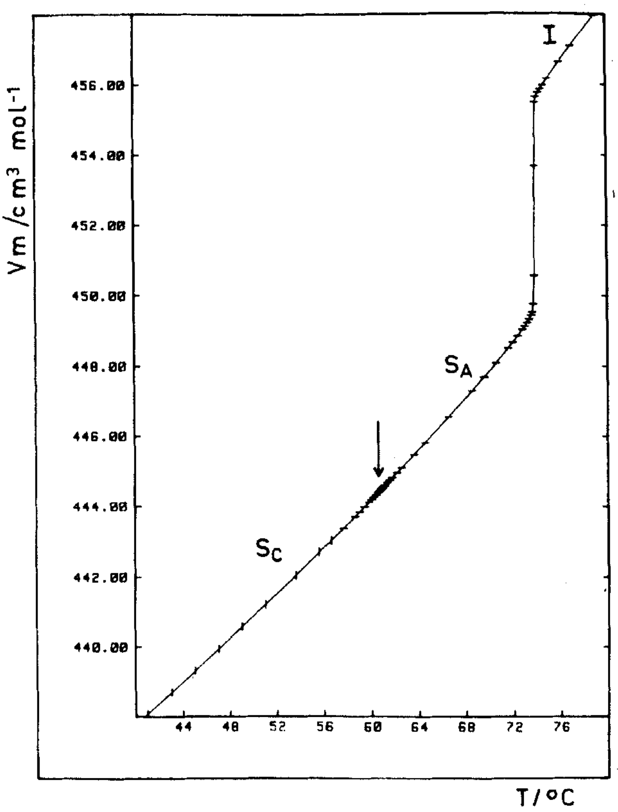

Figure 2. The molar volume $V_m$ of PYP 909 as a function of temperature. The arrow marks the temperature where the $S_C$–$S_A$ transition occurs.

corresponding volume change may be about an order of magnitude smaller. However, some care has to be taken in this comparison as smaller temperature intervals have been chosen for PYP 907 (and PYP 709) resulting in a corresponding lower signal-to-noise ratio for $\alpha$. The expansion coefficient for the $S_C$–$S_A$ transition of PYP 909 is presented on a larger scale in figure 5(*a*) for a heating and a cooling run. No volumetric hysteresis was detectable within our measuring accuracy. In contrast to later results the thermal expansion coefficient $\alpha$ does not change essentially across the phase transition ($\alpha(S_C) \approx \alpha(S_A)$). Note that this phase transition could not be detected definitely by the Perkin-Elmer DSC 2 system [24]. This demonstrates the high sensitivity of our density measurement.

### 3.2. *Comparison of PYP 907 with PYP 709*

Figure 3 shows the molar volumes of PYP 907 and PYP 709 which possess the same molecular mass but interchanged alkyl chain lengths. In the isotropic phase their molar volumes differ by only up to $7 \times 10^{-3}$ per cent. However, surprisingly in the $S_C$ and the $S_A$ phase the packing density of PYP 907 is 0·29 per cent higher than that of PYP 709. What may be the cause for this remarkable behaviour? First, the lateral forces stabilizing the smectic layers might be more attractive for PYP 907 than for PYP 709 as the latter forms at first a nematic phase before the $S_A$ phase is established. This would suggest a higher density for PYP 907 in accord with our experimental

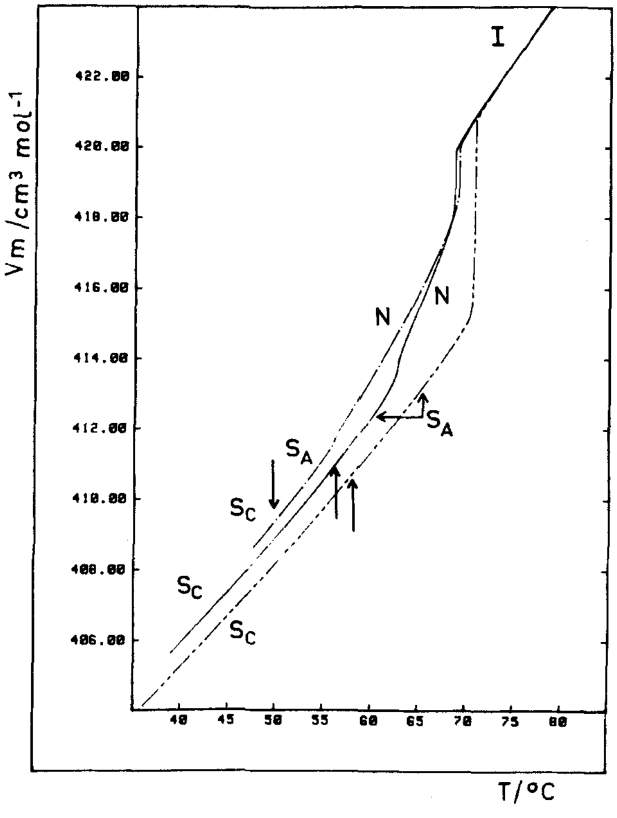

Figure 3. The molar volumes $V_m$ of PYP 709 (–·–·), PY 808 (——) and PY 907 (- - - -).

result. Besides this, the packing density within the smectic layer may be different for PYP 907 and PYP 709. As the molecular ordering is apolar our result means that a high packing density is favoured by symmetric alkyl chain lengths taking the oxygen atom into consideration in estimating the alkyl chain length. The thermal expansion coefficient $\alpha$ of PYP 709 is shown in figure 4 (*c*). The $S_C$–$S_A$ transition is recognizable by a small step in $\alpha$ with $\alpha(S_C) > \alpha(S_A)$. This transition seems to be second order as the volume changes continuously across the transition recognizable by the step in $\alpha$; no coexistence region of $S_C$ and $S_A$ phases could be observed. Moreover the calorimetric study showed a shoulder also indicating of a second order $S_C$–$S_A$ transition. The shape of $\alpha$ across the $S_C$–$S_A$ transition seems to be different from that of PYP 909 given in figure 4 (*a*) but the comparison suffers from the neighbouring crystalline-$S_C$ transition of PYP 709.

The $S_A$-nematic phase transition of PYP 709 is accompanied by strong pre-transitional behaviour in the $S_A$ as well as in the nematic phase preventing us from giving data for the volume change. The first order phase transition nematic–isotropic shows a relative volume jump $\Delta V/V_{NI}$ of 0·42 per cent.

### 3.3. *Comparison of PYP 907 and PYP 709 with PYP 808*

PYP 808 has the same molecular mass as PYP 907 and PYP709 but it is an even numbered homologue of the pyrimidine series. The molar volume of PYP 808 is also

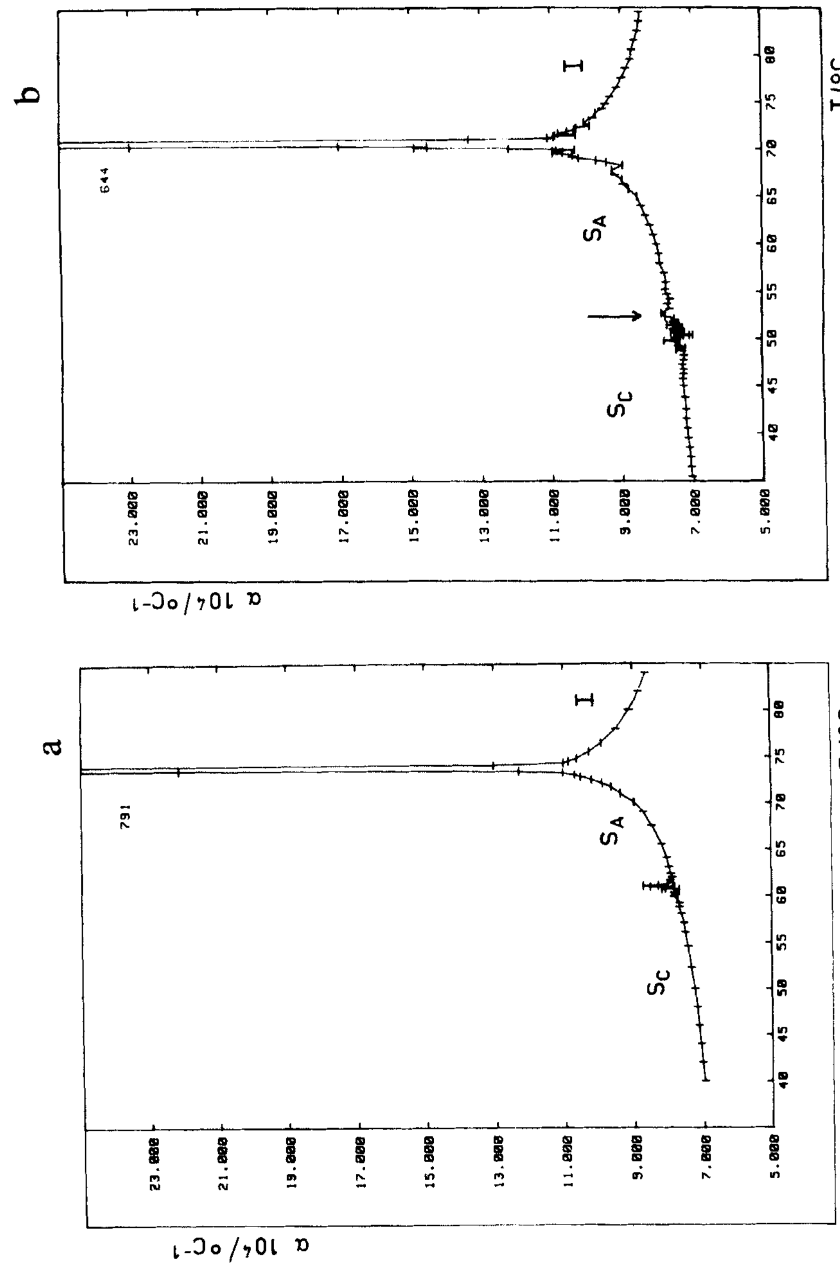
b
644
I
S_A
S_C
T/°C
α 10⁴/°C⁻¹
40
45
50
55
60
65
70
75
80
5.000
7.000
9.000
11.000
13.000
15.000
17.000
19.000
21.000
23.000
a
791
I
S_A
S_C
T/°C
α 10⁴/°C⁻¹

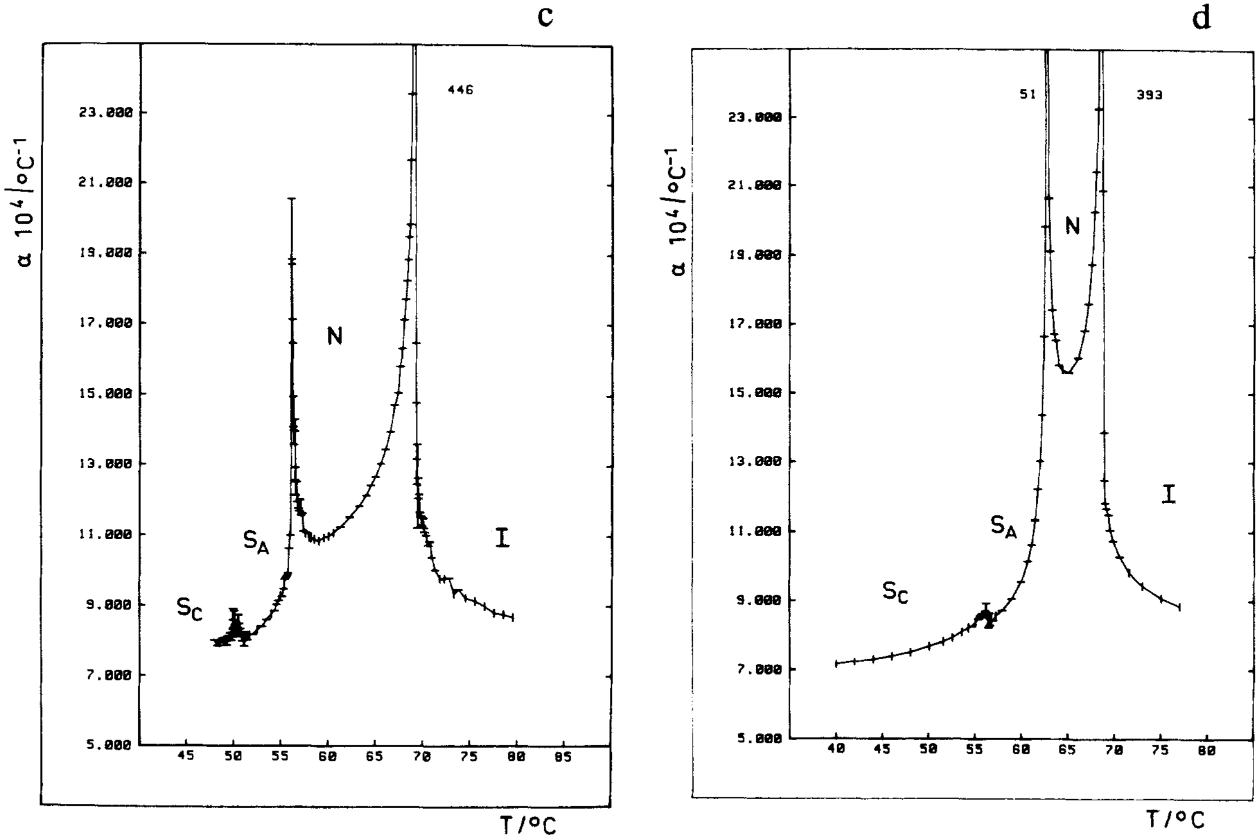

Figure 4. The thermal expansion coefficient $\alpha$ as a function of temperature for (*a*) PYP 909, (*b*) PYP 907, (*c*) PYP 709 and (*d*) PYP 808. In order to see the relevant $S_C$–$S_A$ transition in more detail the vertical axis is considerably extended, cutting off the strong peaks for $\alpha$ at $25 \times 10^{-4}$. The maximum values of these peaks are always given by numbers written next to the peaks. Note that the temperature resolution for PYP 709 and PYP 907 is a factor of two higher, resulting in a correspondingly worse signal-to-noise ratio.

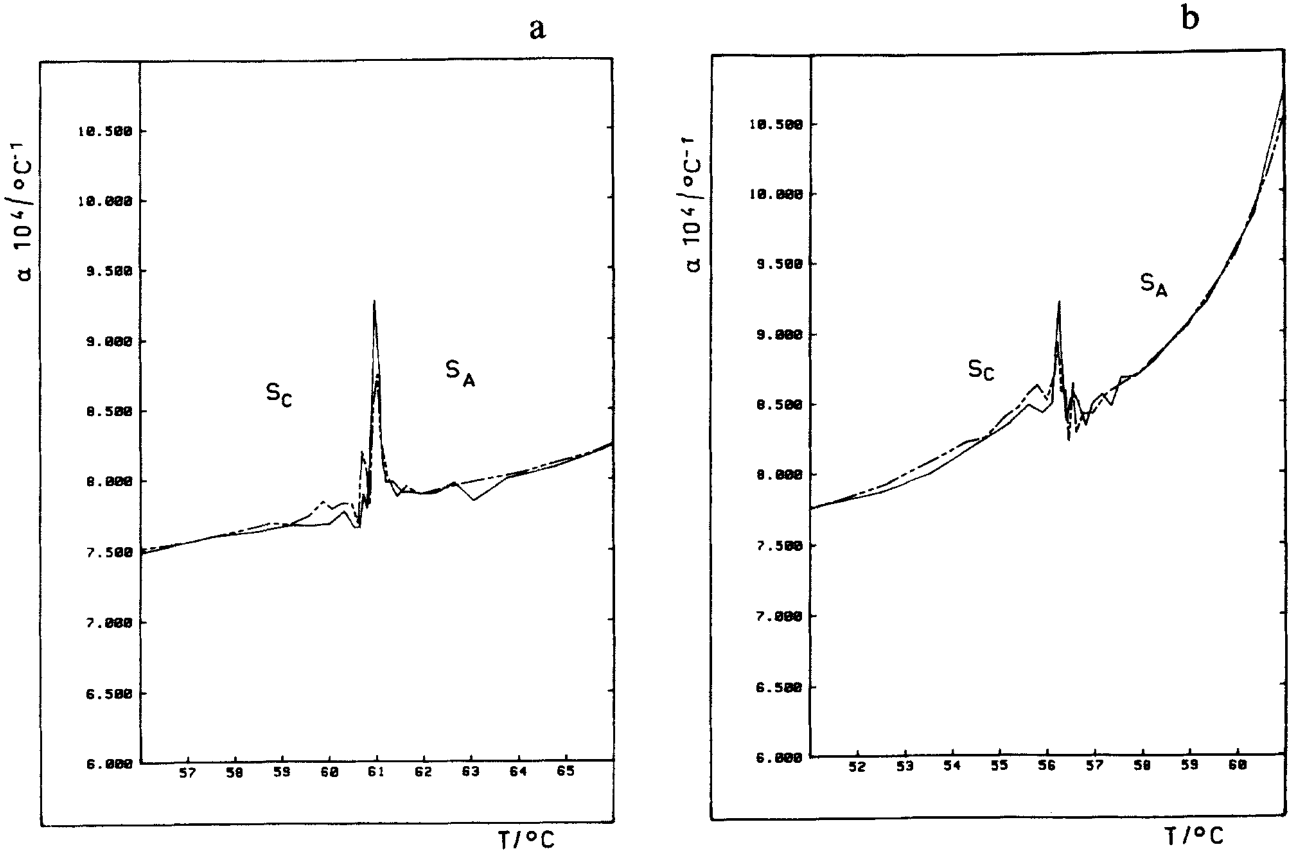

Figure 5. Thermal expansion coefficient α across the $S_A$-$S_C$ transition for (*a*) PYP 909 and (*b*) PYP 808 given on a larger scale for a heating (——) and a cooling (– – –) run. No volumetric hysteresis is observed.

shown in figure 3 and it agrees in the isotropic phase with that of PYP 709 up to $1 \times 10^{-6}$. In the smectic C phase however a considerable deviation appears and the molar volume of PYP 808 lies between the molar volumes of PYP 709 and PYP 907. Assuming that the symmetry of the alkyl chain lengths plays the dominant role for the molecular packing and disregarding odd–even effects PYP 808 should exhibit a lower molar volume than PYP 709 as the alkyl chain lengths are more symmetric in the former case in accord with our experimental observation. A problem arises if PYP 808 is compared with PYP 907. Including again the oxygen atom in the alkyl chain both PYP 808 and PYP 907 possess the same asymmetry in their chain lengths and both contain respectively an even numbered and an odd numbered chain. Accordingly their corresponding molar volumes should be comparable in contrast to the results in figure 3. In fact the two alkyl chains cannot be treated in the same way. The oxygen and the pyrimidine–benzene core break the assumed symmetry leading to sophisticated differences in their molecular interactions. The fact that PYP 808 forms first a nematic phase shows us that the laterally attractive forces should be weaker in this case than for PYP 907. This could, at least qualitatively, explain why the molar volume of PYP 808 is a little larger than that of PYP 907.

By comparing figures 4 (*d*) and (*c*) we realize that the expansion coefficients across the $S_C$–$S_A$ transition for PYP 808 and PYP 709 are of similar shape. We observe in figure 4 (*d*) again a small step with $\alpha(S_C) > \alpha(S_A)$. Figure 5 (*b*) shows $\alpha$ for the $S_C$–$S_A$ transition of PYP 808 on a larger scale for a heating and a cooling run; no volumetric hysteresis could be detected. As is shown in figure 6 (*b*) the volume changes per unit temperature are slightly different below and above the phase transition as indicated by the straight broken lines. The molar volume changes continuously across the $S_C$–$S_A$ transition and no coexistence region of $S_A$ and $S_C$ phases could be observed. Therefore the transition appears to be of second order. This transition was again not detectable with a Perkin–Elmer DSC 2 system.

The relative volume discontinuity $\Delta V/V_{NI}$ of PYP 808 at the nematic–isotropic transition amounts to 0·37 per cent and has a comparable magnitude to that of PYP 709. The volume change of PYP 808 across the $S_A$–nematic transition is about a factor of two larger than that of PYP 709 but both are difficult to determine due to strong pretransitional effects.

### 3.4. *The mixture PYP 708/PYP 706 which possesses a $S_C$–nematic transition*

The molar volume and the corresponding expansion coefficient of the mixture PYP 708/PYP 706 are depicted in figures 7 (*a*) and (*b*). The relative volume jump, $\Delta V/V_{NI}$, at the nematic–isotropic transition amounts to 0·38 per cent and is comparable with that of PYP 808 and PYP 709. The $S_C$–nematic transition is clearly seen as a narrow peak in figure 7 (*b*) with an associated volume discontinuity $\Delta V/V_{S_CN}$ of $2{\cdot}3 \times 10^{-2}$ per cent (see figure 6 (*c*)) which is a factor of 10 larger than $\Delta V/V_{S_CS_A}$ for the $S_C$–$S_A$ transition of PYP 909. The transition exhibits virtually no pretransitional behaviour and seems to be first order according to DSC measurements and the appearance of a two phase region at the $S_C$–nematic transition temperature by a microscopy observation.

### 3.5. *NCB 84—a material which possesses a smectic G phase*

The molar volume and the expansion coefficient of NCB 84 are shown in figures 8 (*a*) and (*b*). The nematic–isotropic phase transition has not been investigated. The

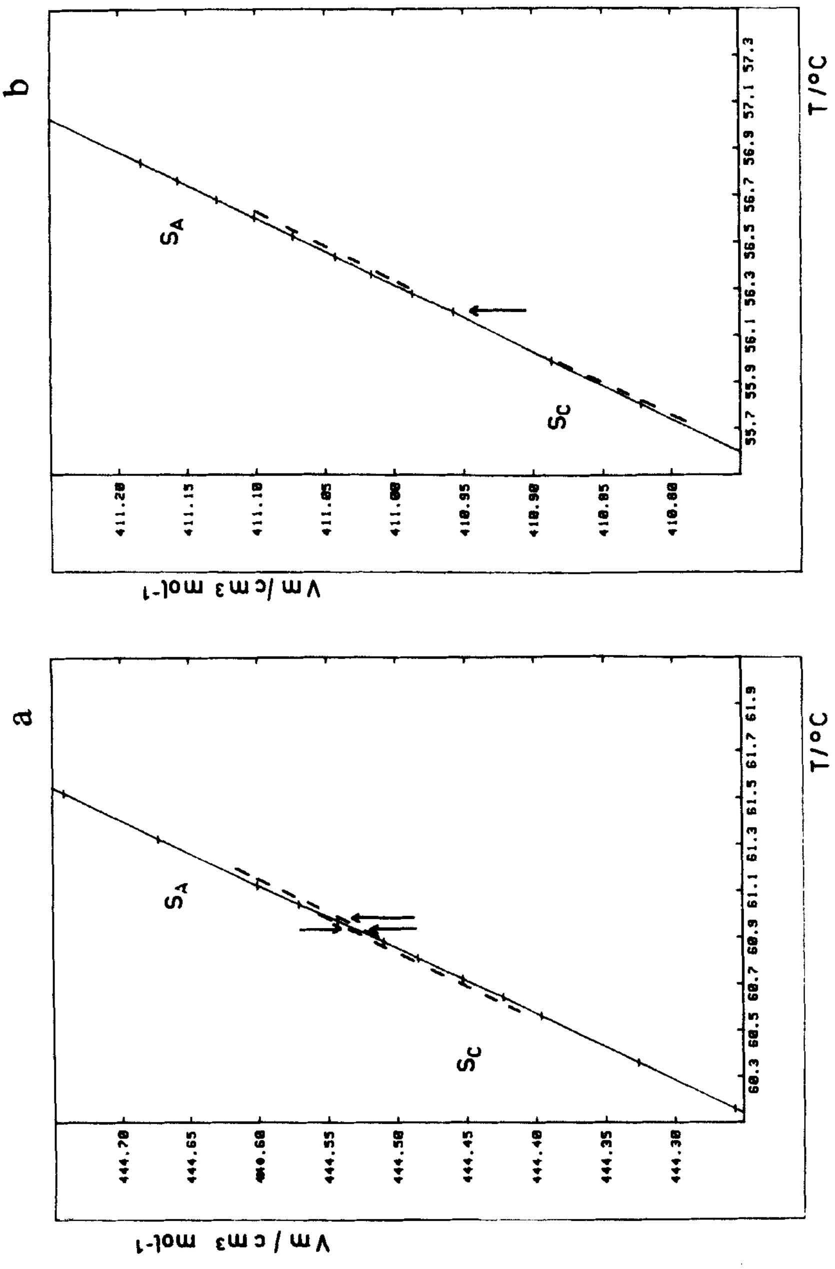
b
V m /c m3 mol-1
411.20
411.15
411.10
411.05
411.00
410.95
410.90
410.85
410.80
T /°C
55.7 55.9 56.1 56.3 56.5 56.7 56.9 57.1 57.3
SA
SC
a
V m / c m3 mol-1
444.70
444.65
444.60
444.55
444.50
444.45
444.40
444.35
444.30
T /°C
60.3 60.5 60.7 60.9 61.1 61.3 61.5 61.7 61.9
SA
SC

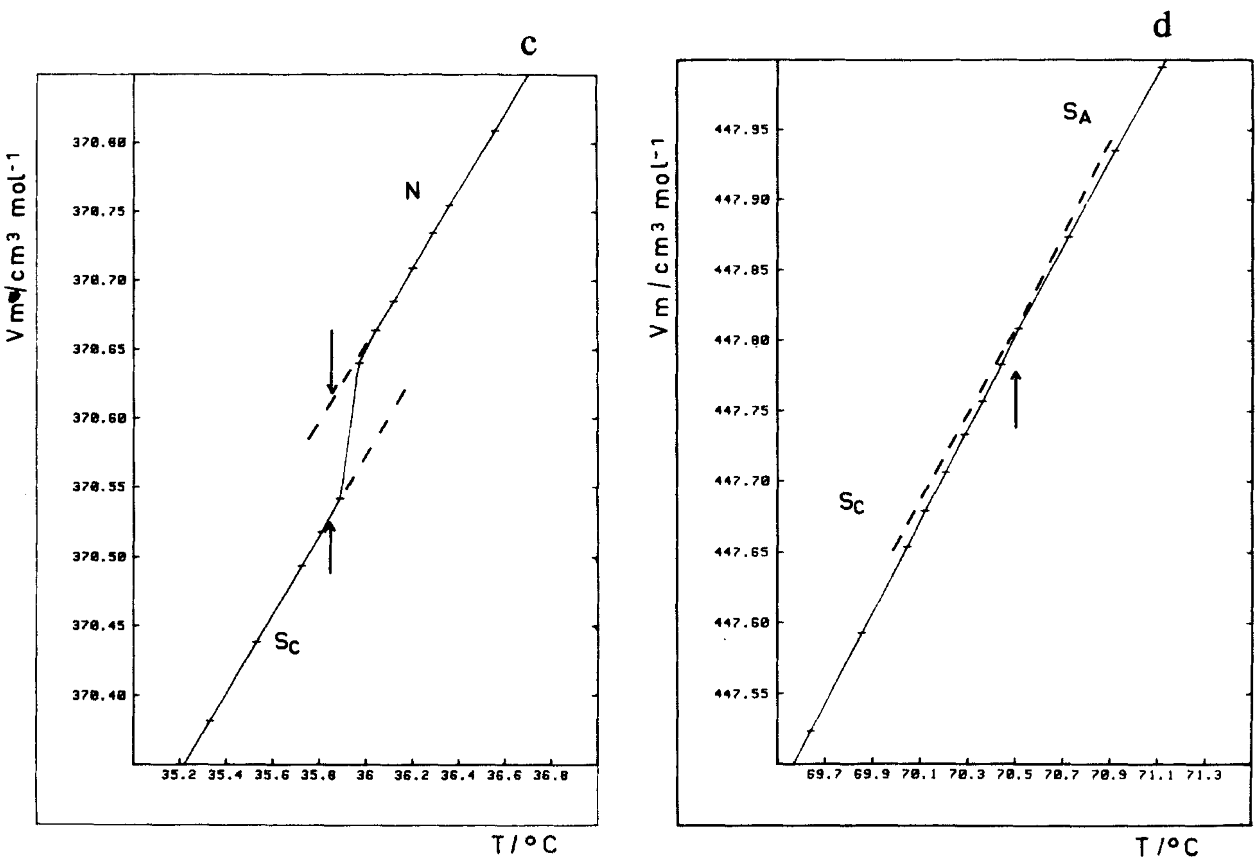

Figure 6. The molar volume $V_m$ as a function of temperature for (*a*) PYP 909, (*b*) PYP 808, (*c*) 48 per cent PYP 708 + 52 per cent PYP 706 and (*d*) NCB84. In order to see the volume change across the relevant $S_C$–$S_A$ ($S_C$–N) transition a section of figures 2, 3, 7 and 8 (*a*) is shown on a larger scale.

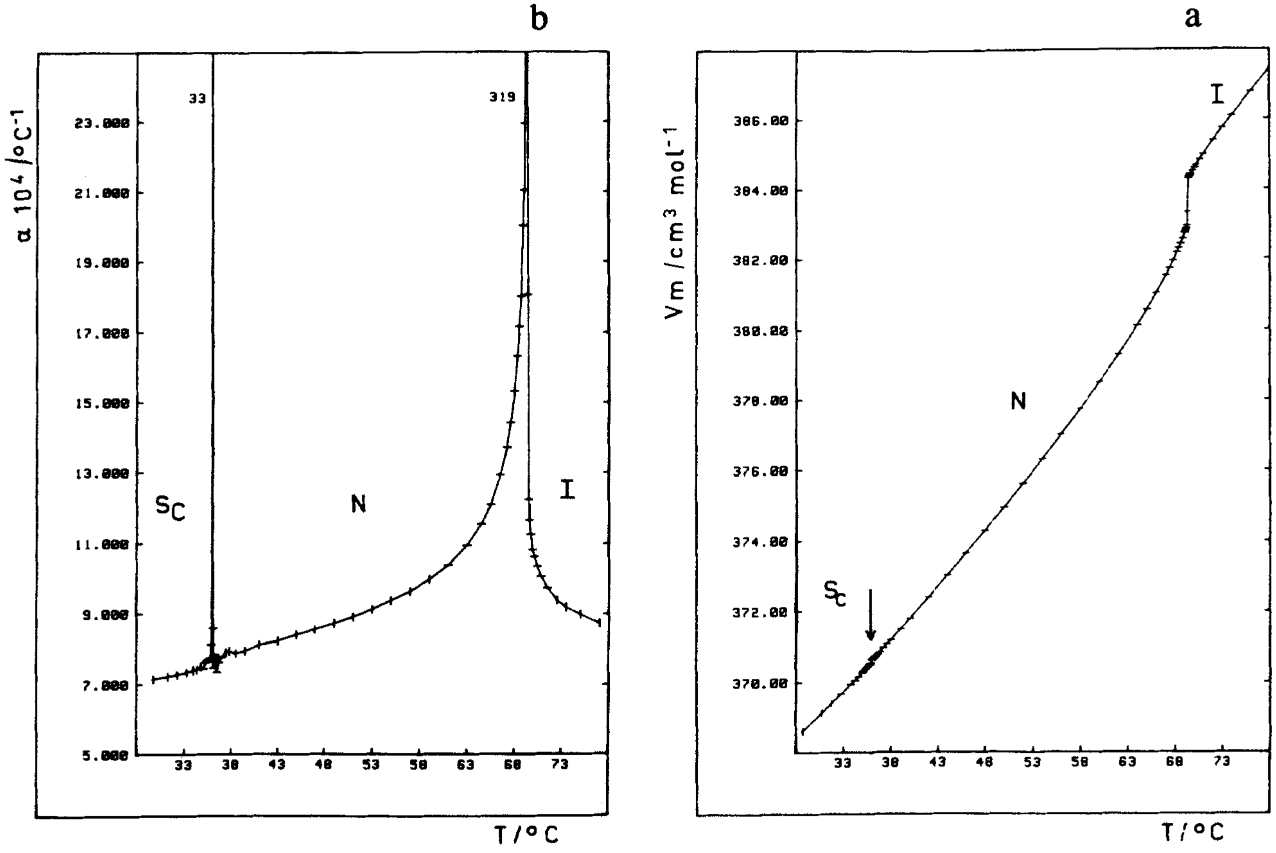

Figure 7. The molar volume $V_m$ as a function of temperature for the binary pyrimidine mixture 48 per cent PYP 708 + 52 per cent PYP 706. (*b*) The thermal expansion coefficient $\alpha$ as a function of temperature for the binary pyrimidine mixture of 48 per cent PYP 708 + 52 per cent PYP 706.

transition from the nematic to the $S_A$ phase is accompanied by strong pretransformations in $\alpha$ and shows a relative volume change $\Delta V/V_{S_A N}$ of $8 \times 10^{-2}$ per cent. The phase transition from the $S_C$ to the $S_A$ phase is recognizable in figure 8 (*b*) by a small step in $\alpha$. The corresponding molar volume across the transition is presented in figure 6 (*d*) on a larger scale. The broken lines indicate that the volume changes per unit temperature are distinctly different in the $S_C$ and the $S_A$ phases and that the transition occurs with a continuous volume change. Moreover the absence of a two phase region and the DSC study [24] point to a second order $S_C$–$S_A$ phase transition. The expansion coefficient is of a similar shape to that for PYP 808 and PYP 709 and the relation $\alpha(S_C) > \alpha(S_A)$ holds again.

At the $S_G$–$S_C$ phase transition a large volume change occurs. A two phase coexistence region was observed across the transition indicating a first order $S_G$–$S_C$ transition. The measurement was not continued to lower temperatures because the viscosity in the $S_G$ phase becomes so high that the measuring precision is strongly diminished. For this reason we have not completed the study of this transition but we can estimate, approximately, a lower limit of 0·7 per cent for the volume change $\Delta V/V_{S_G/S_C}$. The $S_G$–$S_C$ transition exhibits only weak pretransitional behaviour on approaching the $S_G$ phase from above.

By completing the results reported in §§3.1–3.6 we want to emphasize once more the remarkable points concerning the $S_C$–$S_A$ transition. For PYP 709, PYP 808 and NCB 84 we ascertain a continuous volume change and a step of the thermal expansion coefficient $\alpha$ with $\alpha(S_C) > \alpha(S_A)$ both indicating a second order $S_C$–$S_A$ transition. For PYP 909 this transition is probably also of second order but on the other hand the relation $\alpha(S_C) \approx \alpha(S_A)$ holds and no step in $\alpha$ but a cusp-like behaviour is observed which can be interpreted as a discontinuous volume change.

### 3.6. *Influence of a chiral dopant on the phase transitions $S_C$–$S_A$ and $S_C$–nematic*

In order to induce ferroelectric $S_C^*$ phases all $S_C$ materials, with the exception of PYP 907, were doped by the chiral pyrimidine PYP A62Cl which is shown in figure 1. Common to all guest–host mixtures is that the molar volume decreases with increasing content of the chiral dopant. This result seems reasonable for the following reason. From the comparison of the pyrimidine homologues PYP 907, PYP 709, PYP 808 and PYP 606 [25] we can conclude that the molar volume diminishes with decreasing average alkyl chain length, disregarding odd–even effects which are of minor importance. As the average alkyl chain lengths of PYP A62Cl are short in comparison with the non-chiral pyrimidines given in figure 1 the molar volume of the chiral dopant should be distinctly lower. In conclusion also the average molar volumes of the guest–host mixtures should be smaller than those of the pure host compounds assuming ideal mixtures. However, it is worthwhile seeing how the average molar volumes of the various mixtures are influenced by the chiral dopant in a different manner. These results are summarized in figure 9 where the relative volume changes, $-\Delta V/V_0$, are given as a function of temperature. $V_0$ is the molar volume of the pure host, as shown in figures 2, 3, 7 (*a*) and 8 (*a*), and $\Delta V$ is the difference between the average molar volume of the mixture and the molar volume of the pure basis component. It is not a molar excess volume because the molar volume of the chiral dopant is not known and cannot be determined at temperatures below 84°C with our equipment. Clearly the variation of $-\Delta V/V_0$ is largest for NCB84 which possesses the greatest molecular mass. In the same way as the molecular mass (and molar volume)

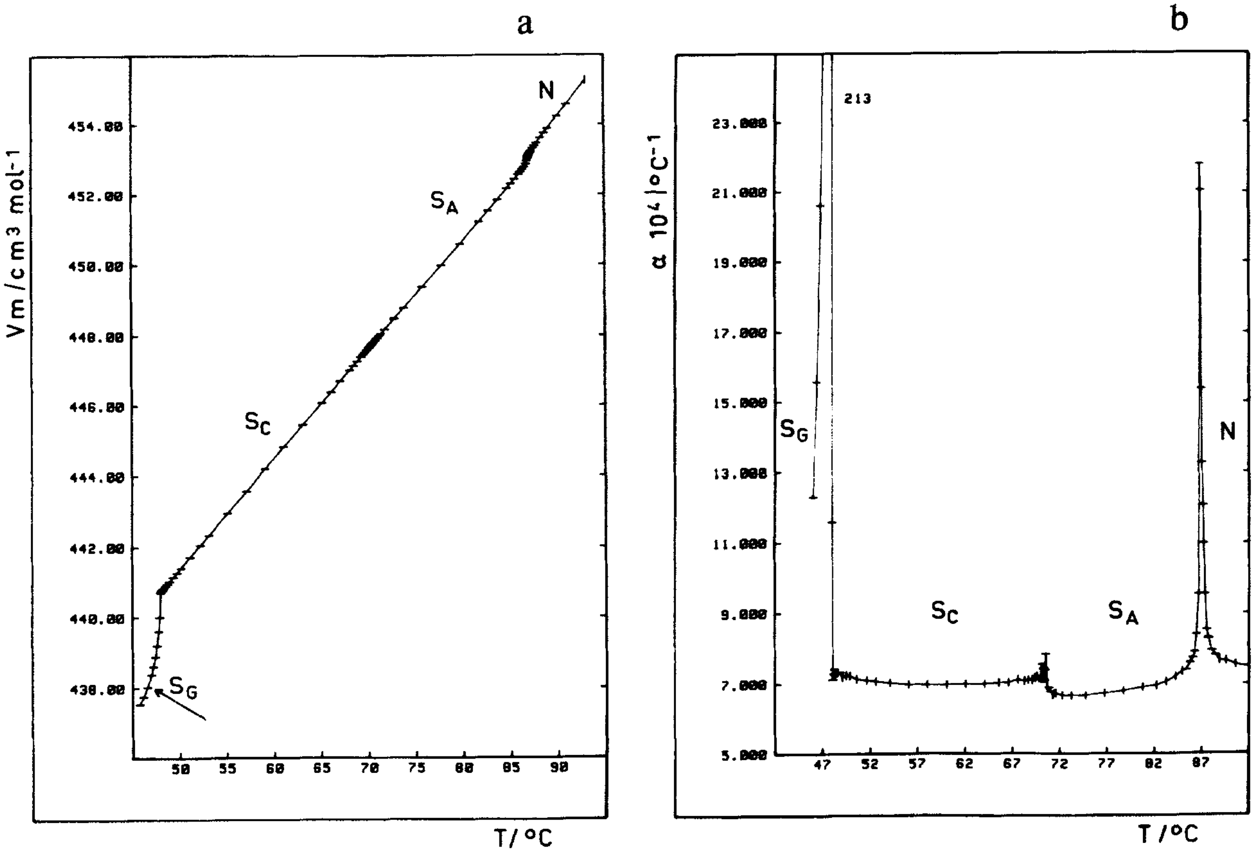

Figure 8. (*a*) The molar volume $V_m$ of NCB84 as a function of temperature. (*b*) The thermal coefficient $\alpha$ for NCB84 as a function of temperature.

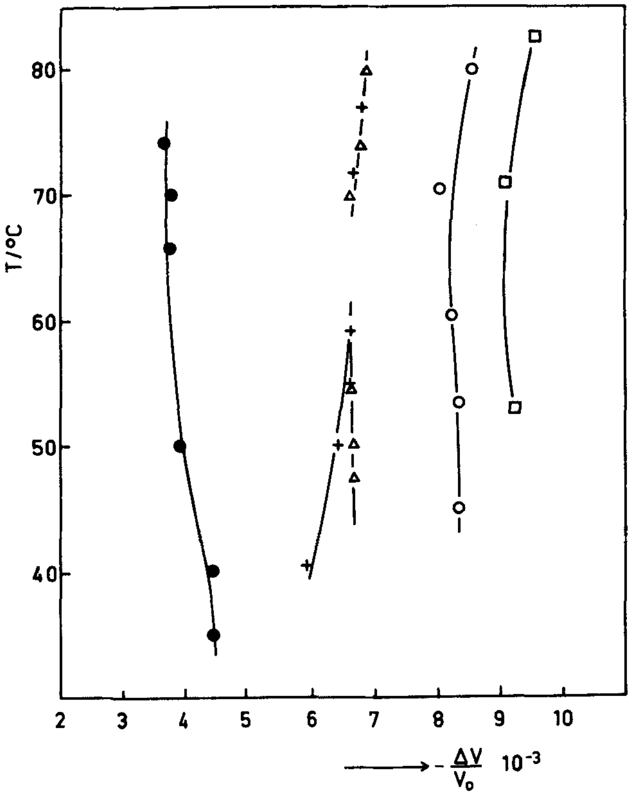

Figure 9. The relative volume changes $-\Delta V/V_0$ as a function of temperature of the non-chiral host substances, given in figure 1, by doping with 2·5 per cent (per weight) of the chiral dopant PYP A62Cl. (●) PYP 708/706, (+) PYP 808, (△) PYP 709, (○) PYP 909 and (□) NCB84.

becomes lower in the sequence PYP 909, PYP 709 (PYP 808) and PYP 708/PYP 706, the quantity $-\Delta V/V_0$ decreases. Therefore the diminution of $-\Delta V/V_0$ is to a first approximation correlated with the molecular mass difference between host and guest molecules. It should be noted that the curves given in figure 9 show only the main features. Near the phase transition considerable deviations may occur which have been omitted from this figure. Instead of presenting the volumetric data of all guest-host mixtures showing always a similar behaviour we have restricted ourselves to the data for PYP 909 for two dopant concentrations, as illustrated in figure 10. Beside the reduction of the average molar volume all transition temperatures (except $S_C$-nematic, see table 1) decrease on adding the chiral dopant. As the chiral dopant has no liquid-crystalline phase it behaves like an impurity which destabilizes the liquid-crystalline phases lowering the transition temperatures. For the pyrimidine hosts the magnitude of the displacement of the transition temperatures is always a factor of three to four larger for the $S_C$–$S_A$ transition than for the nematic-isotropic, $S_A$-isotropic, and the $S_A$-nematic transition. However we shall concentrate on the $S_C$–$S_A$ transition. In figures 11 (*a*)–(*d*) the influence of the chiral dopant on the thermal expansion coefficient of the various host substances is given in a larger scale. The figures contain $\alpha$ for the non-chiral host and $\alpha$ for the guest-host mixture with 2·5 per cent chiral guest dopant. Starting with PYP 909, figure 11 (*a*) shows very

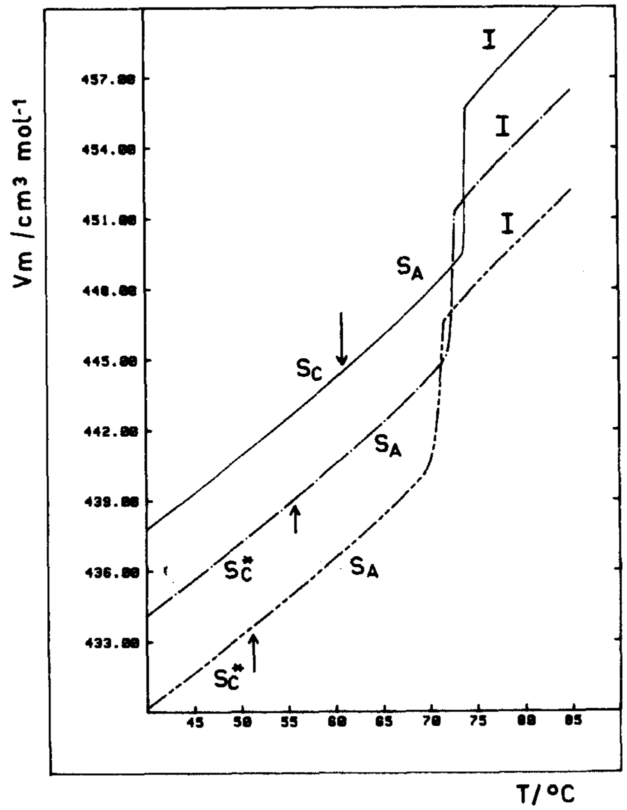

Figure 10. The molar volume $V_m$ as a function of temperature for PYP 909 (——), PYP 909 + 2·5 per cent PYP A62Cl (–·–·) and PYP 909 + 5 per cent PYP A62Cl (– – – – –). The arrows mark the temperature where the $S_C(S_C^*)$–$S_A$ transition occurs.

impressively how adding the chiral dopant diminishes and broadens the peak at the $S_C$–$S_A$ transition. The associated volume change $\Delta V/V_{S_C^*S_A}$ decreases with growing content of the chiral dopant. With 5 per cent of chiral dopant the $S_C^*$–$S_A$ peak is strongly smeared out. On the other hand for PYP 709 the shape of $\alpha$ across the transition is essentially preserved, as shown in figure 11 (*b*).

PYP 808 exhibits very interesting behaviour as shown in figure 11 (*c*). By adding 2·5 per cent of the chiral dopant the step of $\alpha$ across the $S_C$–$S_A$ transition almost completely disappears and a superposed peak is observed which is equivalent to a relative volume change for $\Delta V/V_{S_C^*S_A}$ of $5 \times 10^{-3}$ per cent.

For NCB84 as shown in figure 11 (*d*) we do not observe any difference in the shapes of $\alpha$ on crossing the $S_C^*(S_C)$–$S_A$ transition. A remark should be made about the considerable splitting of the peaks at the $S_C(S_C^*)$–$S_A$ transition shown in figures 11 (*a*)–(*d*). This might be caused by the bad signal-to-noise ratio of $\alpha$ at the phase transition. When the phase transition is crossed the average temperature fluctuation of 0·004°C due to the temperature regulation procedure and the temperature step of 0·08°C lead to a mean error of about 5 per cent in $\alpha$. Figure 11 shows that this is the correct order of magnitude. Far away from the phase transition the large temperature interval of 2°C reduces the error of $\alpha$ to 0·5 per cent.

The $S_C$–nematic ($S_C^*$–Ch) transition of PYP 708/PYP 706 exhibits a peculiarity which is depicted in figure 12. This transition is the only one for which the transition

Volumetric data of the liquid crystal components shown in figure 1 and the ferroelectric mixtures containing respectively 2·5 per cent of the chiral dopant PYP A62Cl. In addition the displacement of the transition temperatures by the dopant as determined by the density measurement are presented; observations by DSC and polarizing microscope are included.

| Liquid crystal compound or mixture | Phase transition | | | | | | DSC | Microscopic observation |
|---|---|---|---|---|---|---|---|---|
| | N–I | $S_A$–N | $S_C$–$S_A$ | $S_A$–I | $S_C$–N | $S_G$–$S_C$ | | |
| PYP 909 | — | — | $\Delta V/V \sim 2 \times 10^{-3}\%$<br>$\alpha(S_C) \approx \alpha(S_A)$ | $\Delta V/V = 1{\cdot}37\%$ | — | — | $S_C$–$S_A$ not clearly detectable | No two phase region at $S_C$–$S_A$ |
| + 2·5% PYP A62Cl | — | — | $\Delta V/V$ decreases<br>$\Delta T = -5{\cdot}7°C$ | $\Delta V/V = 1{\cdot}32\%$<br>$\Delta T = -1{\cdot}2°$ | — | — | Not studied | |
| PYP 907 | — | — | $\Delta V/V \approx 0$<br>$\alpha(S_C) \approx \alpha(S_A)$ | $\Delta V/V = 1{\cdot}35\%$ | — | — | Not studied | No two phase region at $S_C$–$S_A$ |
| PYP 709 | $\Delta V/V = 0{\cdot}42\%$ | $\Delta V/V$ not precisely to determine | $\Delta V \sim 0$<br>step of $\alpha$ with<br>$\alpha(S_C) > \alpha(S_A)$ | — | — | — | $S_C$–$S_A$ detected as second order transition | No two phase region across $S_C$–$S_A$ |
| + 2·5% PYP A62Cl | $\Delta V/V$ unchanged<br>$\Delta T = -1{\cdot}3°C$ | $\Delta T \approx 0$ | $\Delta V \sim 0$<br>$\alpha$ unchanged<br>$\Delta T = -4{\cdot}0°C$ | — | — | — | Not studied | |
| PYP 808 | $\Delta V/V = 0{\cdot}37\%$ | $\Delta V/V$ not precisely determined | $\Delta V \sim 0$<br>$\alpha(S_C) > \alpha(S_A)$ | — | — | — | $S_C$–$S_A$ not detectable | No two phase region at $S_C$–$S_A$ |
| + 2·5% PYP A62Cl | $\Delta V/V$ unchanged<br>$\Delta T = -1{\cdot}4°C$ | $\Delta V/V$ unchanged<br>$\Delta T = -1{\cdot}0$ | $\Delta V/V \sim 5 \times 10^{-3}\%$<br>shape of $\alpha$ changes<br>$\alpha(S_C) \approx \alpha(S_A)$<br>$\Delta T = -3{\cdot}8°C$ | — | — | — | Not studied | |
| PYP 708/PYP 706 | $\Delta V/V = 0{\cdot}38\%$ | — | — | — | $\Delta V/V = 2{\cdot}3 \times 10^{-2}\%$ | — | $S_C$–N first order | Two phase region at $S_C$–N |
| + 2·5% PYP A62Cl | $\Delta V/V$ unchanged<br>$\Delta T = -1{\cdot}1°C$ | — | — | — | $\Delta V/V = 1 \times 10^{-2}\%$<br>$\Delta T = +1°C$ | — | Not studied | |
| NCB 84 | Not studied | $\Delta V/V \approx 8 \times 10^{-2}\%$ | $\Delta V \approx 0$<br>step of $\alpha$ with<br>$\alpha(S_C) > \alpha(S_A)$ | — | — | $\Delta V/V > 0{\cdot}7\%$ | $S_G$–$S_C$ first order<br>$S_C$–$S_A$ second order | Two phase region at $S_G$–$S_C$, but not at $S_C$–$S_A$ |
| + 2·5% PYP A62Cl | Not studied | $\Delta V/V \approx 6 \times 10^{-2}\%$<br>$\Delta T = -2{\cdot}45°C$ | $\Delta V \approx 0$<br>$\alpha$ unchanged<br>$\Delta T = -2{\cdot}0°C$ | — | — | $\Delta V/V$ unchanged<br>$\Delta T = -1{\cdot}3°C$ | Not studied | |

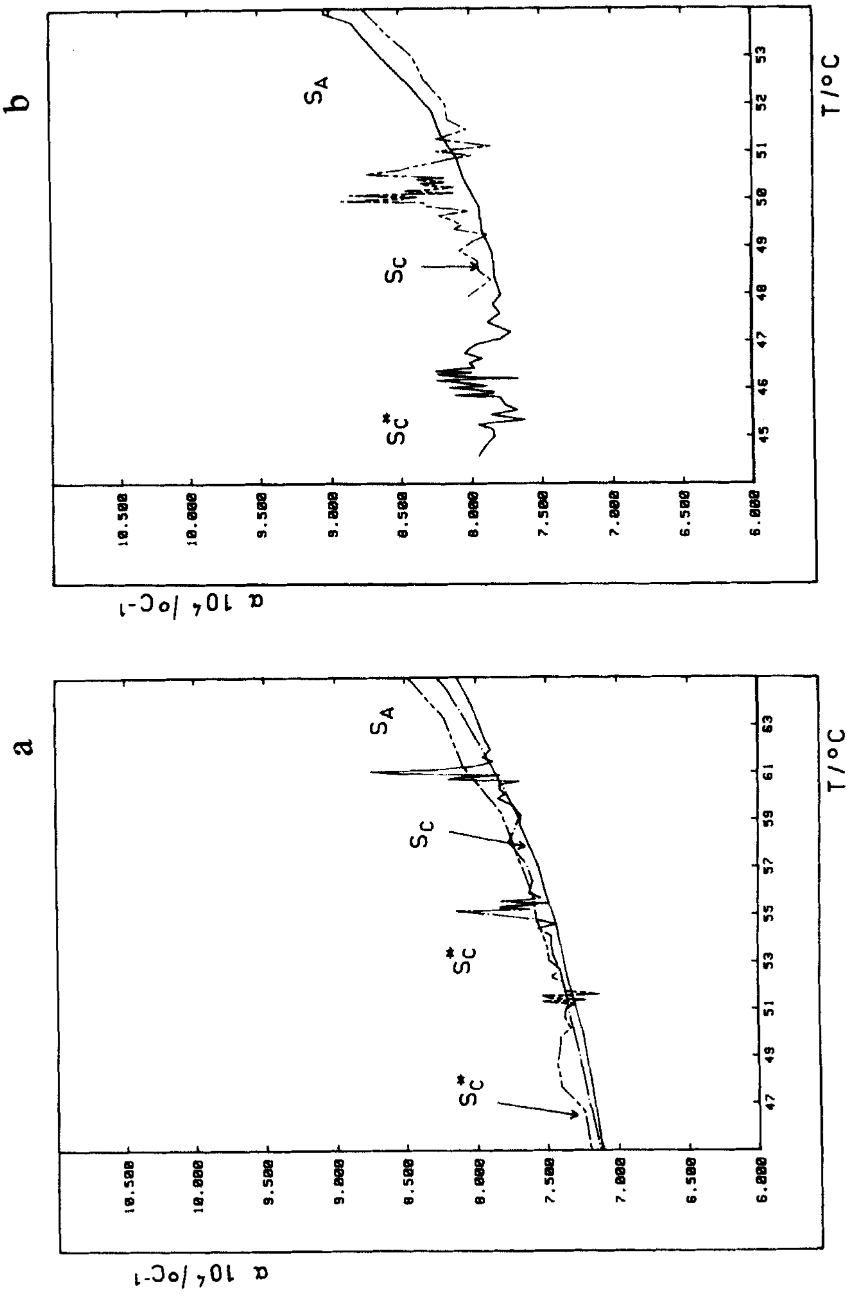
b
α 10⁴ /°C⁻¹
10.500
10.000
9.500
9.000
8.500
8.000
7.500
7.000
6.500
6.000
T / °C
45
46
47
48
49
50
51
52
53
S*C
SC
SA
a
α 10⁴ /°C⁻¹
10.500
10.000
9.500
9.000
8.500
8.000
7.500
7.000
6.500
6.000
T / °C
47
49
51
53
55
57
59
61
63
S*C
S*C
SC
SA

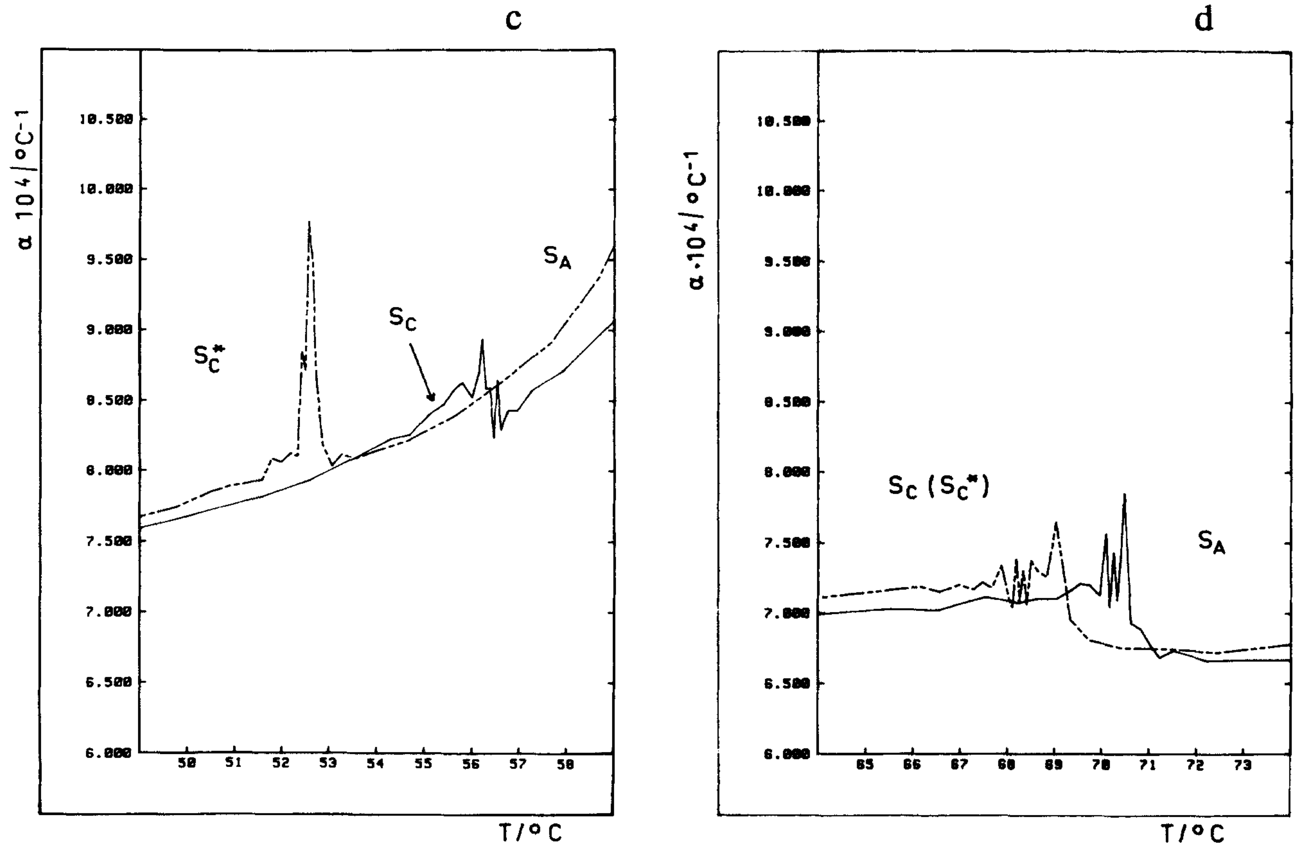

Figure 11. The thermal expansion coefficient α as a function of temperature for (*a*) PYP 909 (——), PYP 909 + 2·5 per cent PYP A62Cl (–·–) and PYP 909 + 5 per cent PYP A62Cl (– – –). (*b*) PYP 709 (– – –) and PYP 709 + 2·5 per cent PYP A62Cl (——). (*c*) PYP 808 (——) and PYP 808 + 2·5 per cent PYP A62Cl (– – –). (*d*) NCB84 (——) and NCB84 + 2·5 per cent PYP A62Cl (– – –).

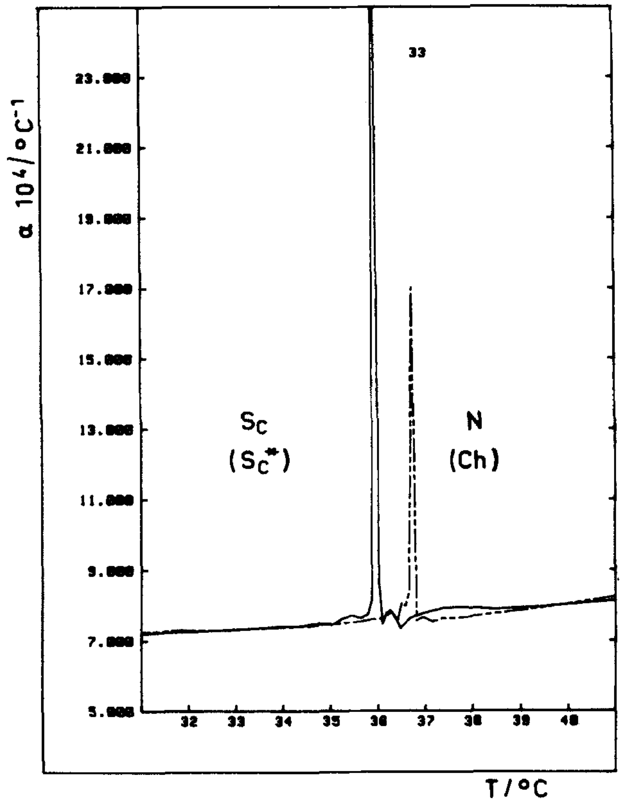

Figure 12. The thermal coefficient α as a function of temperature for the mixture 48 per cent PYP 708 + 52 per cent PYP 705 (——) as well as 46·8 per cent PYP 708 + 50·7 per cent PYP 706 + 2·5 per cent PYP A62Cl (- - -).

temperature increases with growing content of chiral dopant. The volume jump decreases achieving a value for $\Delta V/V_{S_CN}$ of $10^{-2}$ per cent but the sharpness of the transition peak seems to be unchanged.

Summarizing the results given in figures 11 (*a*)–(*d*) in view of the influence of the chiral dopant on the volumetric properties we can subdivide our results in three categories. First for PYP 709 and NCB84 the chiral dopant does not seriously affect the shape of the thermal expansion coefficient across the second order $S_C(S_C^*)$–$S_A$ transition. Secondly a distinct influence of the dopant can be seen for the pyrimidine PYP 909 where the volume change, recognizable by the cusp in α, becomes smaller with increasing dopant concentration. In the third and most interesting case of PYP 808 the continuous $S_C$–$S_A$ transition, indicated by the step of α at the transition, considerably changes its shape by adding of the chiral dopant. A cusp-like behaviour is observed with an associated volume change $\Delta V/V_{S_C^*S_A}$ of $5 \times 10^{-3}$ per cent. But the occurrence of the small volume change need not be caused by the polar interactions responsible for the ferroelectric phase. As is well-known for binary mixtures of liquid crystals with non-mesogenic solutes, the magnitude of the molar volume change may depend on composition and temperature of the mixture [26]. Nevertheless we cannot yet understand why this just happens wth PYP 808. We feel that the dependence of the density on the concentration of the chiral dopant should be investigated in more detail.

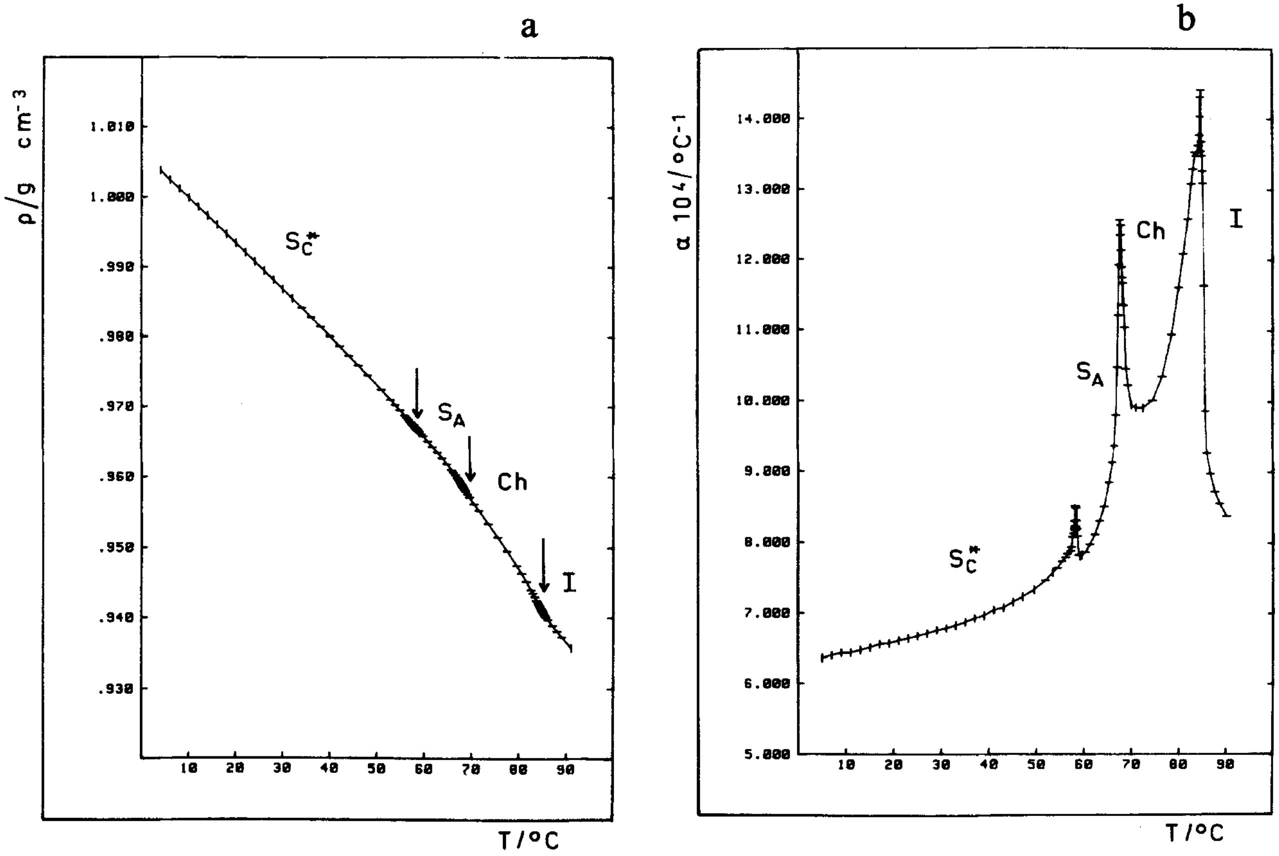

Figure 13. (*a*) The density, $\rho$, as a function of temperature for the ferroelectric broad range mixture ZLI 3488 from Merck. (*b*) The thermal expansion coefficient, $\alpha$, as a function of temperature for ZLI 3488 from Merck.

The table summarizes all of the relevant information on the phase transitions investigated for non-chiral host substances and the chiral doped guest–host mixtures. It is worth comparing the ferroelectric pyrimidine and NCB84 guest–host mixtures with a commercially available ferroelectric mixture. We have measured the density of the broad range mixture ZLI 3488 from Merck as a function of temperature; this has been used in numerous investigations; the result is shown in figure 13 (*a*). A ferroelectric display cell is usually filled in the isotropic phase and cooled slowly down to the $S_C^*$ phase. According to the results in figure 13 (*a*) this is accomplished with an associated density change of about 5–6 per cent which has to be taken into consideration in cell technology. The corresponding thermal expansion coefficient is shown in figure 13 (*b*). The peaks at the Ch–I and $S_A$–Ch transitions are clearly broadened in figure 13 (*b*) due to the many components included in the mixture. Beside the Ch–I and the $S_A$–Ch transition the $S_C^*$–$S_A$ transition is distinctly recognizable in figure 13 (*b*) by the step with the superimposed cusp.

We think that density measurements of smectic phase transitions as described here can give useful complementary information to the common phase transition characterization by microscopic observation and differential scanning calorimetry, especially because of its inherent high sensitivity.

The authors would like to thank Dr. B. S. Scheuble and Dr. T. Geelhaar for supplying the liquid-crystalline materials and Dr. A. E. Stieb for providing us the DSC-data.

## References

[1] DE GENNES, P. G., 1973, *Molec. Crystals liq. Crystals*, **21**, 49.
[2] CLARK, N. A., and LAGERWALL, S. T., 1980, *Appl. Phys. Lett.*, **36**, 899.
[3] LIEN, S. C., HUANG, C. C., and GOODBY, J. W., 1983, *Phys. Rev.* A, **29**, 1371.
[4] SCHANTZ, C. A., and JOHNSON, D. L., 1977, *Phys. Rev.* A, **17**, 1504.
[5] HUANG, C. C., and LIEN, S. C., 1981, *Phys. Rev. Lett.*, **47**, 1917.
[6] HUANG, C. C., and VINER, J. M., 1981, *Phys. Rev.* A, **25**, 3385.
[7] DEHOFF, R., BIGGERES, R., BRISBIN, D., and JOHNSON, D. L., 1981, *Phys. Rev.* A, **25**, 472.
[8] BIRGENEAU, R. J., GARLAND, C. W., KORTAN, A. R., LITSTER, J. D., MEICHLE, M., OCKO, B. M., ROSENBLATT, C., YU, L. J., and GOODBY, J., 1982, *Phys. Rev.* A, **27**, 1251.
[9] MEICHLE, M., and GARLAND, C. W., 1982, *Phys. Rev.* A, **27**, 2624.
[10] HUANG, C. C., and LIEN, S. C., 1984, *Phys. Rev.* A, **31**, 2621.
[11] DEMUS, D., DIELE, S., KLAPPERSTÜCK, M., LINK, V., and ZASCHKE, H., 1971, *Molec. Crystals liq. Crystals*, **15**, 161.
[12] DEMUS, D., and RURAINSKI, R., 1972, *Molec. Crystals liq. Crystals*, **16**, 171.
[13] DEMUS, D., KÖNIG, H., MORZOTKO, D., and RURAINSKI, R., 1973, *Molec. Crystals liq. Crystals*, **23**, 207.
[14] DEMUS, D., and RURAINSKI, R., 1973, *Z. phys. Chem.*, **253**, 53.
[15] RAO, N. V. S., and PISIPATI, V. G. K. M., 1983, *J. phys. Chem.*, **87**, 899.
[16] RAO, N. V. S., and PISIPATI, V. K. G. M., 1984, *Molec. Crystals liq. Crystals*, **104**, 301.
[17] RAO, N. V. S., PISIPATI, V. G. K. M., and GOURI SANKAR, Y., 1985, *Molec. Crystals liq. Crystals*, **131**, 237.
[18] ALAPATI, P. R., POTUKUCHI, D. M., RAO, N. V. S., PISIPATI, V. G. K. M., and SARAN, D., 1987, *Molec. Crystals liq. Crystals*, **146**, 111.
[19] KIEFER, R., and BAUR, G., 1987, *Proceedings of the 17. Freiburger Arbeitstagung Flüssigkristalle.*
[20] ZASCHKE, H., 1980, *Advances in Liquid Crystal Research and Applications*, edited by L. Bata (Pergamon Press), p. 1059.
[21] EIDENSCHINK, R., HOPF, R., SCHEUBLE, B. S., and WÄCHTLER, A. E. F., 1986, *Proceedings of the 16. Freiburger Arbeitstagung Flüssigkristalle.*

[22] Meyer, R. B., 1977, *Molec. Crystals liq. Crystals*, **40**, 33.
[23] Lagerwall, S. T., and Dahl, I., 1984, *Molec. Crystals liq. Crystals*, **114**, 151.
[24] Stieb, A. E. (private communication of unpublished results).
[25] Kiefer, R., and Baur, G. (to be published).
[26] Orwoll, R. A., Rhyne, R. H., Jr., Christensen, S. D., and Young, S. D., 1977, *J. phys. Chem.*, **81**, 181.